AE-285
UDC 536.423.1
621.039.524.46

AE-285

Power Disturbances Close to Hydrodynamic Instability in Natural Circulation Two-Phase Flow

R. P. Mathisen and O. Eklind

AKTIEBOLAGET ATOMENERGI
STOCKHOLM, SWEDEN 1967

POWER DISTURBANCES CLOSE TO HYDRODYNAMIC INSTABILITY IN NATURAL CIRCULATION TWO-PHASE FLOW

by

R. P. Mathisen and O. Eklind

SUMMARY

In certain boiling reactor designs high positive void coefficients could exist and under certain circumstances cause instability. Control systems may therefore be desired. In such a controlled reactor there could remain superimposed low frequency power oscillations of some magnitude. The object of the current experiments in SKÄLVAN was to examine whether or not such slow oscillations could influence the hydrodynamic stability limit of the individual boiling channels.

While operating the loop close to the threshold of hydrodynamic instability, the power was pulsed in the boiling channel. The pulse widths had a lower limit of 0.65 sec due to the contactor time constant. The square wave power oscillation amplitude $\frac{\Delta Q}{Q}$ was 12.2 %, and the interval T between the pulses was varied in the range $0 < \frac{T_o}{T} < 0.5$ where T_o was the mass flow oscillation period. The corresponding mass flow oscillations remained damped for all disturbance periods which were examined.

With minimum test section inlet restrictions the power level at instability was much lower than that at burnout conditions. At higher restrictions these phenomena occurred at approximately equivalent power levels. The experiments with minimum inlet restrictions were also performed beyond the instability threshold. In this case it was possible to exceed the nominal burnout point temporarily by 5 per cent or more for periods of the order of magnitude 1 second. Even now the boiling channel conditions were not so severely affected that the burnout detectors tripped, and the power disturbances caused low frequency modulated wave trains.

Printed and distributed in July 1967.

LIST OF CONTENTS

1. INTRODUCTION

The experiments were performed in order to indicate whether or not the maximum power limit with respect to hydrodynamic instability in natural circulation two-phase flow was influenced by disturbances occurring periodically and with frequencies which were lower than the natural frequency. Although the dynamic behaviour of a boiling loop cannot easily be compared to that of an entire reactor system, the results may give some indications as to whether or not a water cooled reactor, operated fairly close to the hydrodynamic instability limit, may be affected by superimposed low frequency disturbances. Such low frequency oscillations of small amplitude could, for instance, occur in a reactor lying close to void reactivity stability limit. They could also occur in a reactor which would be instable in the absence of a control system, but where a control system is used to counteract the basic instabilities, leaving only a slight residual ripple in the reactor power.

C. L. Spigt (ref. [8]) observed a low frequency resonance peak in his power-to-void transfer functions, experimentally obtained in an out-of-pile natural circulation loop. The actual frequency was about 0.04 cps. He concluded that this coupling could be attributed to intercoupling of the flow process in the boiling channel with that in the condenser which might be more dominant at lower frequencies. At some loop conditions, this type of oscillation totally disappeared. In this connection he mentions that increasing pressure caused this type of oscillation to start at higher power levels. He also states the paradox that increasing the power level sometimes caused the oscillations to stop and in other cases to modulate the higher frequency oscillations. He did not mention the damping effect of for instance inlet restrictions and system driving head.

Preliminary tests in SKÄLVAN showed that power steps or regular square wave power oscillations caused dominating system pressure transients due to small pressurising volume in the loop. To avoid this parameter influence, power disturbances with pulselike character were introduced. For each of the different mean power levels examined, the periods between the pulses were varied in the

range $0 < \frac{T_o}{T} < 0.5$, where T_o is the period of the oscillations at hydrodynamic instability. The results are presented as immediate amplitude response $(\frac{\Delta \dot{m}}{\bar{\dot{m}}})_o / \frac{\Delta Q}{\bar{Q}}$ as well as the mean damping coefficient $\bar{k}$ in the assumed function:

$$\frac{\Delta \dot{m}}{\bar{\dot{m}}} = (\frac{\Delta \dot{m}}{\bar{\dot{m}}})_o \cdot e^{kt} \cdot \sin(\omega_o t) \qquad (1)$$

2. APPARATUS

The loop features are described in previous reports (ref. [1-6]). However, a brief description of the special facilities for power oscillation is reported.

2.1 Power oscillation facilities

The electrically heated test section was coupled in series with the power oscillation equipment which consisted of two water cooled electrical resistances. For minimum power one of these resistances was disconnected while for maximum power both were coupled in parallel by means of a time relay operated air cooled contactor. All types of step disturbance functions could thus be produced. See figs. 1 and B1.

2.2 Instrumentation

A drag-body type strain gauge flowmeter, which was steady-state and dynamically calibrated for the actual frequency range, was mounted at the test section inlet, and a high frequency oscillograph indicated the flow oscillations. See fig. 1.

3. THE POWER OSCILLATIONS

The power oscillating equipment merely allowed square wave types of disturbances. However, sinusoidal power oscillations may be introduced by sinusoidally varying the converter magnetising current.

The square wave system is governed by double sets of time relays. This makes it possible to vary the power oscillation from square wave to pulselike power signals.

Due to the contactor time constants the minimum width of the pulses was about $\Delta t = 0.65$ sec.

The mean heat output varies with the period T between the pulses:

$$\overline{Q} = Q_o + \frac{\Delta t}{T} \cdot \Delta Q_{sq.w.} \tag{2}$$

where

$$\Delta Q_{sq.w.} = Q_{max} - Q_o \tag{3}$$

The equivalent sinusoidal power amplitude

$$\Delta Q_{sin} = \frac{4}{\pi} \cdot \Delta Q_{sq.} \tag{4}$$

4. THE FLOW OSCILLATIONS

If $\overline{\dot{m}}$ is the steady-state mass flow rate corresponding to a certain indicated quantity L, the following expression gives the general relationship:

$$\overline{\dot{m}} = C(\vartheta)\,(k \cdot L^n + c) \tag{5}$$

Using the derivative of this function also for finite perturbations, the relative oscillations are expressed by

$$\frac{\Delta \dot{m}}{\overline{\dot{m}}} = n \cdot \frac{\Delta L}{L} \tag{6}$$

if the zero output mass flow rate c is negligible. The flowmeter was calibrated in accordance with this relationship (ref. [5]) for the following ranges:

$0 < f < 4$ cps

$0.33 < \overline{\dot{m}} < 1.67$ kg/sec

$0.09 < \frac{\Delta \dot{m}}{\overline{\dot{m}}} < 0.9$

The flow response to any power disturbance was sinusoidal and may hypothetically be expressed:

$$\eta = \frac{\Delta \dot{m}}{\bar{\dot{m}}} = \left(\frac{\Delta \dot{m}}{\bar{\dot{m}}}\right)_o \cdot \exp(kt) \cdot \sin(\omega_o t) \tag{7}$$

where $\left(\frac{\Delta \dot{m}}{\bar{\dot{m}}}\right)_o$ is the immediate maximum amplitude, and k is the damping constant. Due to non-linearities the lapse is not purely exponential. However, solving k according to eq. (7) we get

$$k = \frac{\ln\left(\frac{\eta}{\eta_o}\right)}{t} - \frac{\ln \sin(\omega_o t)}{t} \tag{8}$$

Selecting $t = \frac{2n-1}{4} T_o$, where n is a convenient integer common for all cases examined, the calculated $\bar{k}$ assumed fairly representative values, which were not affected significantly by the power disturbance frequency.

5. CHOICE OF LOOP CONDITIONS

The following loop characteristics were chosen:

1.	Nominal system pressure	$P = 50$ bar
2.	Inlet subcooling	$\Delta\vartheta_s = 8\text{-}10.5\ ^{o}C$
3.	Test section diameter	$D_h = 20$ mm
4.	Test section length	$L_T = 4.3$ m
5.	Riser diameter	$D_R = 46$ mm
6.	Riser length	$L_R = 1.05$ m
7.	Driving head	$H = 5.23$ m
8.	Test section inlet restrictions	$k_o = 1.6$ and 13.0 velocity heads
9.	Relative power oscillation (Square wave)	$\frac{\Delta Q}{Q_o} = 12.2\ \%$

Most of the experiments were performed with minimum test section inlet restrictions in order to reduce the power level at instability and to produce the most vigorous responses to power oscillations. Finally some comparative tests were performed with "normal" inlet restrictions, $k_o = 13.0$ velocity heads. The riser exit throttling was neg-

ligible, e.g. the area ratio outlet to chimney cross section was of order of magnitude 5:1, corresponding to $k_{e.r.} = 0.96$ velocity heads, referred to the boiling channel cross section.

6. EXPERIMENTAL RESULTS

First, the power density Q^*_{cr} at instability was determined experimentally for the chosen loop conditions. With the single channel inlet restrictions $k_o = 1.6$ and 13.0 velocity heads, Q^*_{cr} was 127.5 and 162.5 kW/litre, corresponding to $T_o = 1.575$ and 1.700 sec. respectively. Q^*_{cr} was determined according to the principle shown in fig. A1. The subcoolings were 8 °C in the first and 10.5 °C in the second case. For these cases the burnout points with natural circulation were also determined. Fig. 2 shows the experimental points as well as the predicted instability power and forced circulation burnout as functions of the inlet throttling. These curves were calculated in accordance with Becker's round duct correlation and appendix A.

Obviously, the forced circulation data were high compared to the natural circulation burnout points. This can be explained as follows. According to fig. A4 the chosen subcooling gives relatively low instability power level. There exists a firm relationship between the instability and the burnout in natural circulation, and thus the burnout points were rather low in this case. Fig. 2 also shows the maximum power disturbance levels which could be raised more than 5 % over the actual burnout power level for periods of about 1 second and still not affect the boiling channel conditions so vioently that the burnout detectors tripped. The mass flow and pressure response to ± 12.2 % square wave power step variations are shown in fig. 3: a) from different to equal power levels, b) from equal to different power levels. When ΔQ was negative, the corresponding mass flow oscillations were more damped than for positive ΔQ. The system pressure transients were quite dominating and the power steps caused considerable changes in the operating conditions.

As the object of these experiments was to examine whether or not the power level at hydrodynamic instability was influenced by power disturbances with any frequency lower than the resonance frequency, it was convenient to introduce pulselike perturbations to minimise

the influence of pressure transients, and to start the investigations with loop conditions disposed for distinct responses to any disturbance.

Typical mass flow response to pulselike disturbances at the relative power levels $\overline{Q}/Q^*_{cr} = 0.93$, 0.96 and 0.99 for P = 50 bar, $\Delta\vartheta_s = 8\ ^oC$ and $k_o = 1.6$ velocity heads are shown in fig. 4.

Pulselike power disturbances were also introduced when the loop was operated beyond the power level at instability. Fig. 5 shows typical loop behaviour at the relative power level $\overline{Q}/Q^* = 1.04$. In this case the corresponding mass flow perturbations were low frequency modulated wave trains, the amplitudes of which sooner or later assumed the initial constant value. By varying the periods between the pulses, relative flow response amplitudes as shown in fig. 6 were obtained at the relative power levels $\overline{Q}/Q^*_{cr} = 0.93$, 0.96 and 0.99. Fig. 6 shows the results for $k_o = 1.6$ velocity heads over a narrow spectrum. It was obvious that the amplitude peaks appeared at integral multiples of the resonance frequency period T_o. For the case $\overline{Q}/Q^*_{cr} = 1.04$, the period T was also varied. For relatively short disturbance periods the loop behaviour was quite similar to that when power pulses were introduced below the instability level, as one could imagine by considering the first time inerval in fig. 5.

The amplitude maxima over the frequency range $0 < \frac{T_o}{T} < 0.5$, both for $k_o = 1.6$ and 13.0 velocity heads are shown in fig. 7. In the case $k_o = 13.0$ v.h. it was not possible to raise the relative power level to more than $\overline{Q}/Q^*_{cr} = 0.96$ before the burnout detectors tripped, disturbed by the pulses. In fact the power pulse maxima in this case were almost 7 % beyond the natural circulation burnout point (see fig. 2).

The mean damping coefficient $\overline{k}$ versus $\overline{Q}/Q^*_{cr}$ is shown in fig. 8. The corresponding mass flow oscillations were not damped significantly by increasing the inlet restrictions.

7. CONCLUSIONS

Introducing repeated power disturbances, changes the operating conditions of the boiling channel periodically. It will be difficult to ana-

lyse the experimental data using the assumption that the process is linear, particularly when the power level is gradually raised beyond the critical power.

The experiments showed that the hydraulic instability power level was not influenced by any power disturbance frequency in the range, even when the power during the pulses was raised considerably over the nominal natural circulation burnout point.

Even for $\overline{Q} = 1.04\ Q^{*}_{cr}$, $k_o = 1.6$ velocity heads, the boiling channel conditions were not so severely influenced by the power pulses that the burnout detectors tripped. In this case the corresponding mass flow wave trains were modulated by varying low frequencies. These wave trains assumed a quasi-damped character when the power disturbance frequency increased.

The resonance frequency variation with power was negligible in the cases examined. Increasing inlet restrictions had no significant damping effect on the system in terms of the mean damping coefficient $\overline{k}$.

8. ACKNOWLEDGEMENTS

The authors wish to thank Mr. Jan Flinta and Mr. Nicolaas Schuch for stimulating and valuable discussions, and Mr. Harry Kurtmar who has been working tenaciously to get consistent results.

9. REFERENCES

1. MATHISEN R P, HERNBORG G and VALKING L,
1963. AB Atomenergi, Sweden. (Internal report. RPL-641.)

2. BECKER K M, MATHISEN R P, EKLIND O and NORMAN B,
Measurements of hydrodynamic instabilities, flow oscillations and burnout in a natural circulation loop.
Nukleonik, 6 (1964) 224-233.

3. BECKER K M, JAHNBERG S, HAGA I, HANSSON P T and MATHISEN R P,
Hydrodynamic instability and dynamic burnout in natural circulation two-phase flow. An experimental and theoretical study.
International conference on the peaceful uses of atomic energy, Geneva 3. 1964. Geneva 1965. Proc. Vol. 8, p. 325.

4. HANSSON P T, MATHISEN R P and EKLIND O,
1964. AB Atomenergi, Sweden. (Internal report. RTL-759, RFR-291.)

5. MATHISEN R P,
1964. AB Atomenergi, Sweden. (Internal report. RTL-760.)

6. MATHISEN R P and EKLIND O,
An experimental study of natural circulation in a loop with parallel flow test sections. 1965.
(AE-200.)

7. MATHISEN R P,
1965. AB Atomenergi, Sweden. (Internal report. TPM-RTL-830.)

8. SPIGT C L,
On the hydraulic characteristics of a boiling water channel with natural circulation. 1966.
(WWO 16-R 92.)

9. BECKER K M,
A correlation for burnout predictions in vertical rod bundles. 1966.
Euratom. Symposium on boiling crisis in two-phase flow systems. ISPRA, June 14-17, 1966. 1966.
(S-349.)

10. EKLUND R, GELIUS O, HERNBORG G, NYLUND O and ÅKERHIELM F,
Fröja. FT-6b. Experiments performed during August 66. Results. 1966.
ASEA, Sweden. (Internal report. KAB 66-25.)

11. EKLUND R, GELIUS O, HERNBORG G, NYLUND O and ÅKERHIELM F,
Fröja. FT-6b. Experiments performed during October 66. Results. 1966.
ASEA, Sweden. (Internal report. KAB 66-27.)

APPENDIX A

The power level at instability in natural circulation two-phase flow. Empirical functions

In accordance with the plotting technique shown in fig. A1, experimental data of the power density at hydrodynamic instability in round duct test sections were fitted to the parameters which determine the downcomer conditions.

The influence of the downcomer flow restrictions at constant pressure was first obtained. The following cases were investigated:

1. Parallel boiling channels with equal inlet restrictions.
2. " " " " unequal inlet restrictions.
3. Single boiling channel.

The following empirical equations cover the three cases, with the allowance that the second case gave slightly higher power density than the two others. The equation obtained from the results reported in ref. [6] fits also other loop data within the accuracy $2s = 5.2\ \%$:

$$Q^*_{cr} = \sigma_k \, Q_{TRH} \tag{A1}$$

where the liquid flow restriction influence is:

$$\sigma_k = k_o^a \cdot \exp\left(\div \frac{k_o + k_v}{b \cdot \exp(c\, k_o)}\right) \tag{A2}$$

k_o stands for the boiling channel initial inlet restrictions and k_v the main flow restrictions in the downcomer, i.e. $k_{in} = k_o + k_v$. The constants according to the experimental data were:

$$a = 0.0968 \qquad b = 68.2 \qquad c = 0.157$$

The most convenient form of eq. (A2) for slide rule calculations is:

$$\sigma_k = \exp\left\{ \frac{\ln k_o}{10.23} - \frac{k_o + k_v}{68.2 \exp(0.157\, k_o)} \right\} \tag{A2}$$

The experimental restriction ratios covered the ranges $1.6 < k_o < 11.6$ and $0 < k_v < 70$ velocity heads of liquid phase, referred to the cross section of one boiling channel.

Ref. [6] states that single- and parallel test sections gave almost similar power levels at hydrodynamic instability provided that the inlet restrictions were equal. According to eq. (A2), the power level at instability concerning parallel boiling channels is improved by increasing the inlet restrictions (k_o) of the channels, while restricting the main flow rate (k_v) has the opposite effect. This is true for completely separated boiling channels.

The substitution of the restrictions k_o and $k_o + k_v$ with the total upstream restriction k_{in} makes eq. (A2) valid also for single test section instability data.

This definition of k_o and k_v, however, may be difficult to use concerning the stability problem in rod cluster types of boiling channels. Probably, the subchannel interaction across the rod bundles will not be suppressed by the introduction of channel inlet restrictions, which, depending on the channel design, may cause effects more or less similar to those of k_v in fig. A2. For the "conventional" rod cluster design of today, the best boiling reactor performance would probably be obtained at fairly low liquid phase restrictions, since it may be doubtful whether the inlet restrictions will give the decided stabilising effect for this channel geometry. The experimental results in ref. [10-11] may, although showing somewhat diverging trends, confirm this suggestion.

The constant Q_{TRH} in eq. (A1) is dependent on the riser and heated channel geometry and flow patterns, as well as the driving head H of the system and may be considered as a boiling channel and riser constant.

The influence of system pressure on the power level at instability has also been established for constant subcooling and varying downcomer restrictions. For $\Delta\vartheta_s = 6\ ^{o}C$ in both single and parallel boiling channels, the following expression is valid:

$$\sigma_\Psi = \Psi^{0.55} \qquad \text{(A3)}$$

where

$$\Psi = \frac{P}{50}, \quad P \text{ in atg.}$$

σ_Ψ is the pressure influence function. See fig. A3.

The pressure was varied in the range $5 < P < 60$ atg experimentally. The empirical equation (A4) for the hydrodynamic instability at constant subcooling $\Delta\vartheta_s = 6\ ^{o}C$ and completely separated boiling channels fits the experimental data within the accuracy $2s = 6.2\ \%$:

$$Q^*_{cr} = \sigma_k \cdot \sigma_\Psi \cdot Q_{TRH} \tag{A4}$$

The influence of inlet subcooling with constant inlet restrictions and varying system pressure was obtained for single channel as well as for parallel channel flow conditions. The power density at instability showed a minimum in the region $10 < \Delta\vartheta_s < 30\ ^{o}C$ depending on the system pressure. An empirical equation of the type

$$\sigma_\vartheta = C_1\ (\vartheta - 1) + C_2 \cdot P + C_3 \tag{A5}$$

seemed to fit the experimental results. Here $\vartheta = \frac{\Delta\vartheta_s}{6}$. The subcooling was varied in the range $4 < \Delta\vartheta_s < 60\ ^{o}C$.

The experiments were repeated for different inlet flow restrictions to obtain the influence of k_o on the coefficients C_1, C_2 and C_3, obtaining:

$$\sigma_\vartheta = \frac{\Delta\vartheta_s \exp\left(\div \frac{P}{25\ k_o^{0.1}}\right)}{22.22\ k_o^{0.34}} + \frac{4.1 \exp\left(\div \frac{\Delta\vartheta_s}{4 \exp\left(\frac{P}{40}\right)}\right)}{P^{0.57}} +$$

$$+ \frac{12.65\ k_o \exp\left(\frac{P}{250}\right) \cdot \exp\left(\frac{k_o}{250}\right) + \ln\left(\frac{P}{40}\right) \exp\left(\frac{\Delta\vartheta_s}{23.5}\right)}{24\ k_o} \tag{A6}$$

The final empirical equation (A7) fits the experimental results obtained so far within the accuracy $2s = 8.4\ \%$:

$$Q^*_{cr} = \sigma_k \cdot \sigma_\psi \cdot \sigma_\vartheta \cdot Q_{TRH} \tag{A7}$$

This equation is valid for the following ranges of the parameters:

$1.6 < k_o < 11.6$ velocity heads of liquid phase
$0 < k_v < 70$ " " " " "
$10 < P < 60$ atg
$4 < \Delta\vartheta_s < 60$ °C

The related σ-functions concern results with constant driving head, boiling channel and riser geometry.

Experimental results, as well as the values for the power density at instability for varying system pressure, inlet subcooling and flow restrictions are shown in fig. A4. In these cases the value of Q_{TRH} was 134.5 kW/litre.

APPENDIX B

The power oscillation system. Electrical characteristics

The following requirements have to be considered in order to dimension the electrical resistances in the power oscillation system:

a. The decided relative magnitude of the power amplitude (± p).

b. The test section power Q_T should be as high as possible.

c. The contactor current I_2 should be as low as possible.

d. The heat flux in the water cooled electrical resistances R_1 and R_2 must not reach critical values.

e. Certain A. C. -converter limitations with respect to voltage and current.

Fig. B1 shows a simple resistance coupling which seems to be the best fit for these requirements, expressed by the following:

a. $$\bar{I}^2 = (1+p) \cdot I_{min}^2 = (1-p)\, I_{max}^2 \qquad (B1)$$

$$\therefore \quad I_{min} = \sqrt{\frac{1-p}{1+p}} \cdot I_{max} = \alpha \cdot I_{max}$$

b. $$Q_T = f(R,\ R_1,\ R_2) \qquad (B2)$$

c. $$I_2 = I_1 \cdot \frac{R_1}{R_2} = I_{max} - I_1 = I_{max} \cdot \frac{R_1}{R_1 + R_2} \qquad (B3)$$

d. $$\left(\frac{Q}{F}\right)_{R_1} = \frac{I_{min}^2 \cdot \rho}{\pi^2 \cdot d_m \cdot \delta\,(d_m - \delta)} = C \cdot I_{min}^2 \qquad (B4)$$

e. $$V = (R_1 + R)\, I_{min} = \left(R + \frac{R_1 R_2}{R_1 + R_2}\right) I_{max} \qquad (B5)$$

Eqs. (B1) and (B5) give:

$$R_2 = \frac{R_1 [(R_1 + R)\, a - R]}{(R_1 + R)(1 - a)} \tag{B6}$$

Normalised to the test section electrical resistance R, the following function

$$R'_2 = \frac{R'_1 [(R'_1 + 1)\, a - 1]}{(R'_1 + 1)\, (1 - a)} \tag{B7}$$

gives a non-dimensional nomographic concept for evaluating the resistances R_1 and R_2 for a given test section electrical resistance R and the chosen power oscillation amplitude p.

Eq. (B7) gives

$$R'_2 = 0 \text{ for } R'_1 = 0 \text{ or } R'_1 = \frac{1 - a}{a}$$

$$\frac{dR_2}{dR_1} = 0 \text{ gives } R'_1 = \frac{\sqrt{a} - a}{a} \quad \text{and} \quad R'_2 = \frac{(1 - \sqrt{a})^2}{a - 1}$$

Since $a < 1$, R'_2 becomes negative for all $R'_1 < \frac{1 - a}{a}$.

For a given a, i.e. a given power oscillation $\pm p$, the relative electrical resistance R'_1 must thus be chosen as $R'_1 \geq \frac{1 - a}{a}$, and the related resistance R_2 must be selected in accordance with eq. (B7) to fulfil other requirements, for instance expressed by the eqs. (B2), (B3) or (B4).

The parallel electrical currents coupled by the contactor are:

$$\frac{I_1}{I_2} = \frac{R_2}{R_1} = \frac{(R_1 + R)\, a - R}{(R_1 + R)(1 - a)} \tag{B8}$$

The test section currents are respectively:

$$I_{min} = I_1 = \frac{V}{R_1 + R}$$

$$I_{max} = I_1 + I_2 = \frac{V}{(R_1 + R)\, a} \tag{B9}$$

eqs. (B8) and (B9) give:

$$I_2 = \frac{1-a}{a} \cdot \frac{V}{R_1} = \frac{R_1}{R_1+R_2} \cdot I_{max} \tag{B10}$$

and

$$I_1 = \frac{[R_1 a - R(a-1)]\, V}{R_1 (R_1+R)\, a} \tag{B11}$$

Eq. (B10) is a hyperbolic function of R_1 while eq. (B11) has a maximum for the resistance value:

$$R_1 = \frac{1-a+\sqrt{1-a}}{a} \cdot R$$

corresponding to $R_2 = R$ in accordance with eq. (B7).

Fig. B1 shows the values R'_1, R'_2, I'_1, I'_2, I'_{min} and I'_{max}, normalised with respect to the test section resistance R and the current $\frac{V}{R}$, where V is the total system voltage. In this case p = 0.1, e.g. the power oscillation becomes $\overline{Q} \pm 10\ \%$.

NOMENCLATURE

A	area	m^2
c	zero output mass flow rate	kg/sec
C	coefficient	
$C(\vartheta)$	temperature dependent coefficient	
D	diameter	mm
f	frequency	sec^{-1}
H	driving head	m
I	electrical current	amp
I'	relative electrical current	
k	flow restriction coefficient	velocity heads
$\overline{k}$	mean damping coefficient	
l	length	m
L	indicator output	varying units
ΔL	indicator output, amplitude	" "
$\dot{\overline{m}}$	mean mass flow rate	kg/sec
$\Delta\dot{m}$	oscillating mass flow amplitude	kg/sec
n	flow power function exponent	
n	integer	
P	system pressure	bars
Q	power	kW, kW/litre
$\overline{Q}$	mean power	" "
Q^*_{cr}	power at hydrodynamic instability	" "
R	electrical resistance	ohm
R'	relative electrical resistance	
s	standard deviation	
t, T	time	sec
V	voltage	volt

Greek letters

α	coefficient	
δ	wall thickness	mm
η	relative amplitude	
ϑ	temperature ratio	
$\Delta\vartheta$	liquid subcooling	^oC

ρ	specific electrical resistance	ohm mm^2 m^{-1}
σ	function	
Ψ	pressure ratio	
ω	angular frequency	rad/sec

Indices

e.r.	exit riser
in	inlet
k	liquid flow restriction
R	riser
s	subcooling
sin	sinusoidal
sq.w.	square wave
T	test section
TRH	unchanged test section, riser and driving head
o	reference - for instance inlet
v	main liquid flow
ϑ	temperature
Ψ	pressure

THE NATURAL CIRCULATION LOOP "SKÄLVAN"

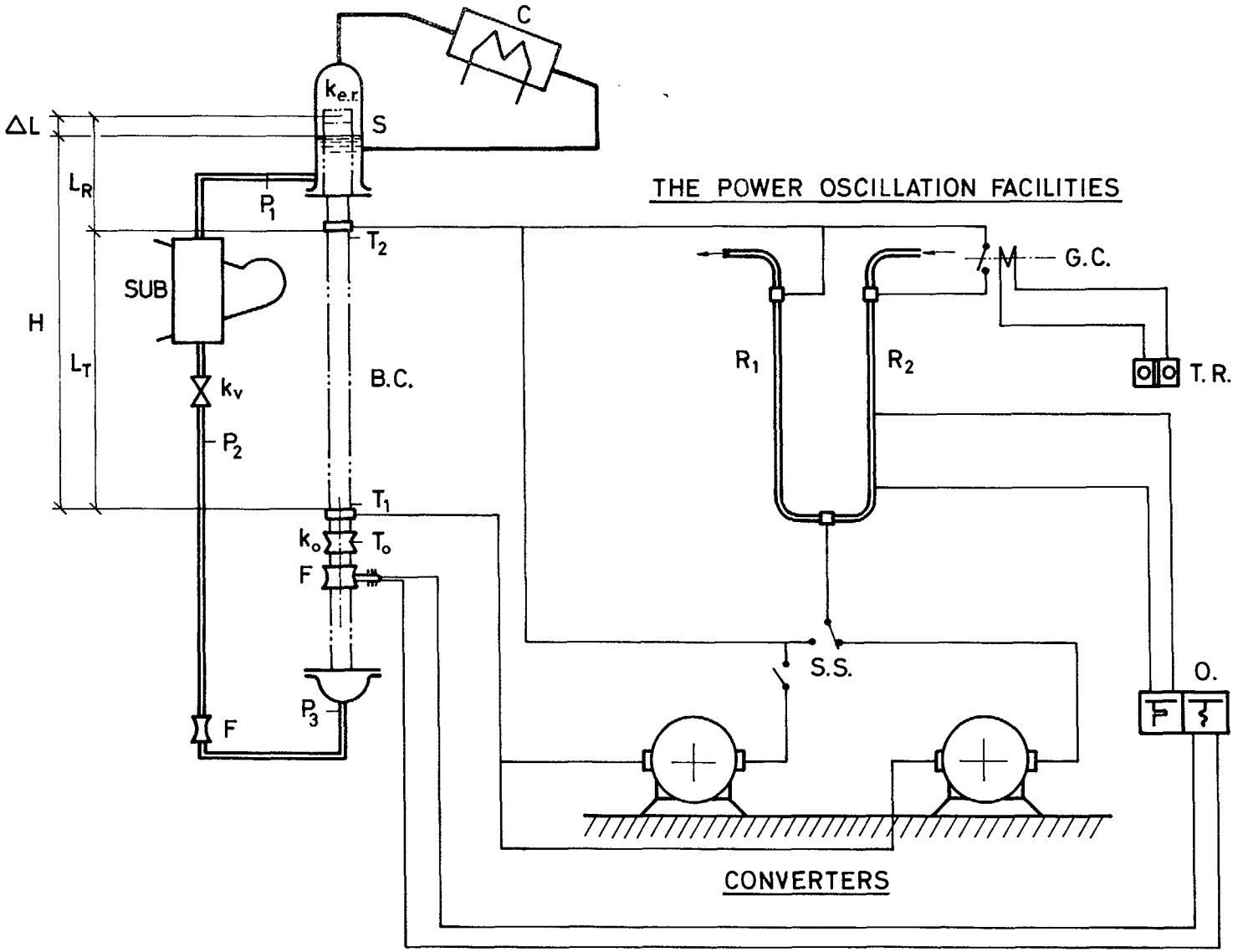

B.C. BOILING SINGLE OR PARALLEL CHANNELS
C CONDENSER
F FLOW METERS
G.C. GUIDED CONTACTOR
H EFFECTIVE HEAD
k THROTTLING DEVICES
L_R RISER LENGTH
L_T TEST SECTION LENGTH
O OSCILLOGRAPH
P PRESSURE TAPS
R WATER COOLED ELECTRICAL RESISTANCES
S STEAM SEPARATOR
S.S. SELECTOR SWITCH
SUB SUBCOOLER
T THERMOCOUPLES
T.R. TIME RELAYS

FIG. 1 FLOW DIAGRAM

LOOP DATA:

P	= 50 bar	H	= 5.23 m
L_T	= 4.30 m	D_T	= 20 mm
L_R	= 1.05 -"-	$k_{e.r.}$	= 0.96 v. h.

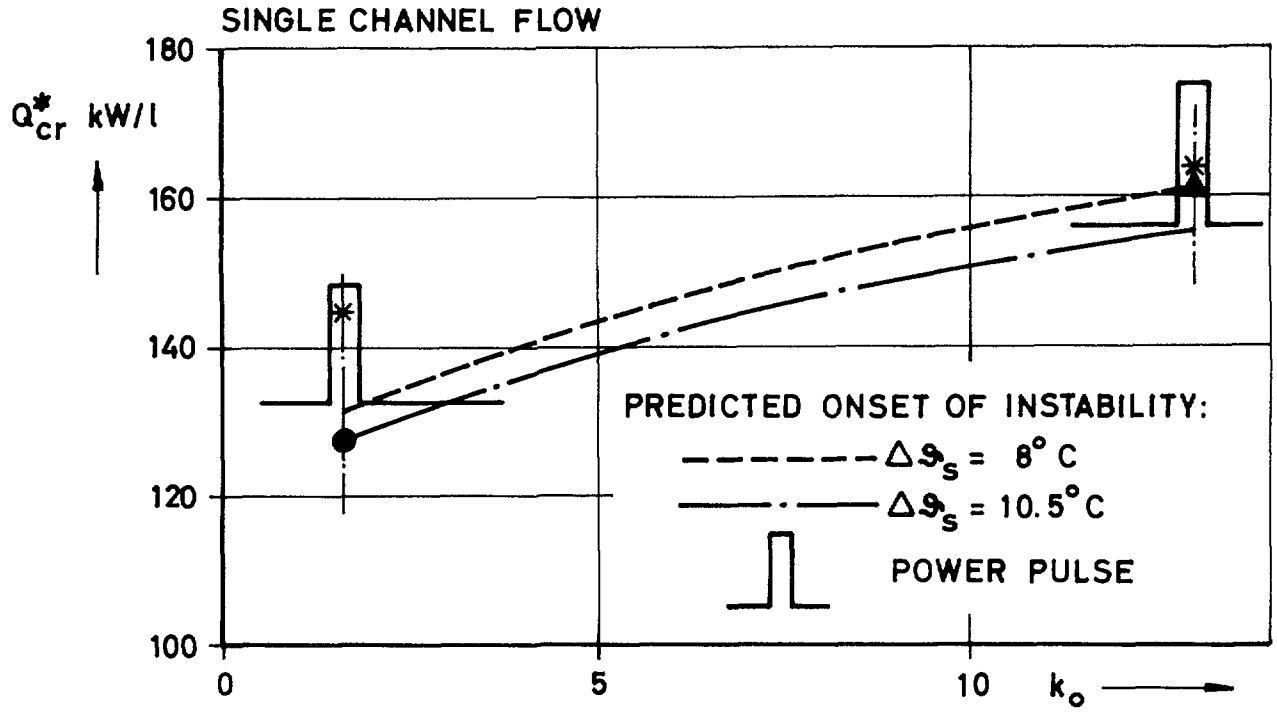

LEGEND:

- ● ONSET OF INSTABILITY, $\Delta\vartheta_s$ = 8° C P = 50 bars
- ▲ -"- -"- -"- $\Delta\vartheta_s$ = 10.5° C P = 50 -"-
- ✱ BURNOUT POINT.

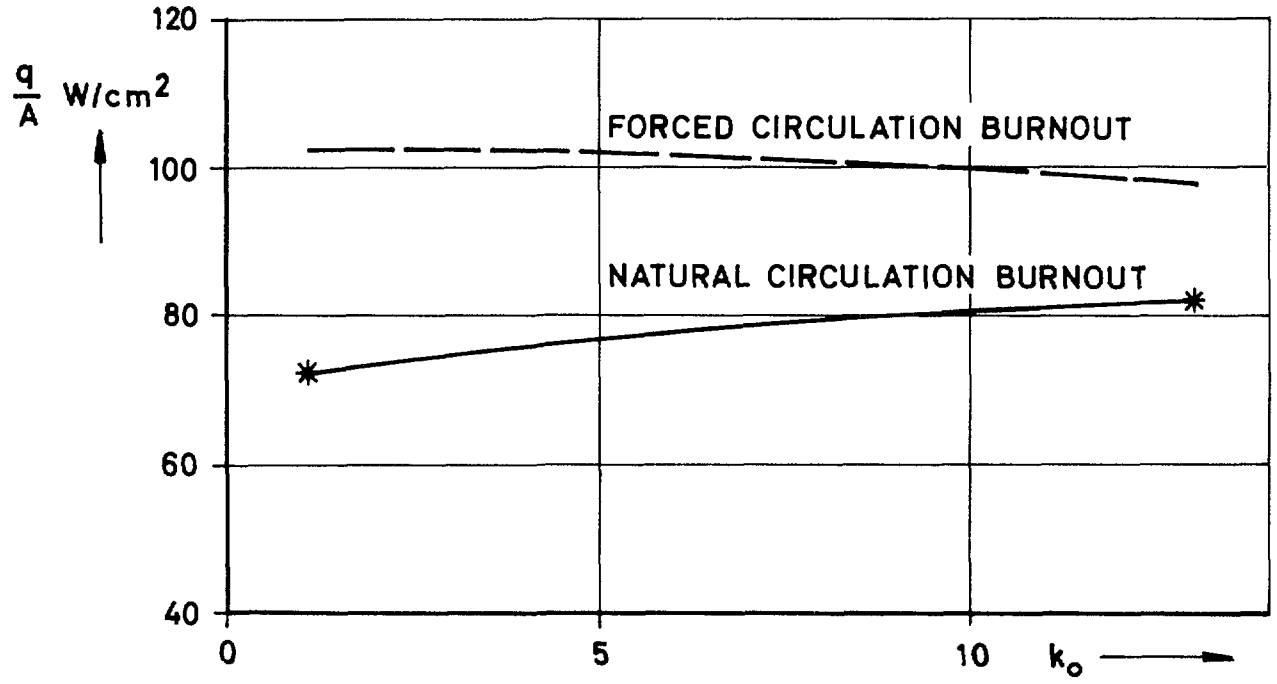

FIG. 2 NATURAL CIRCULATION POWER LIMITS VERSUS TEST SECTION INLET RESTRICTIONS

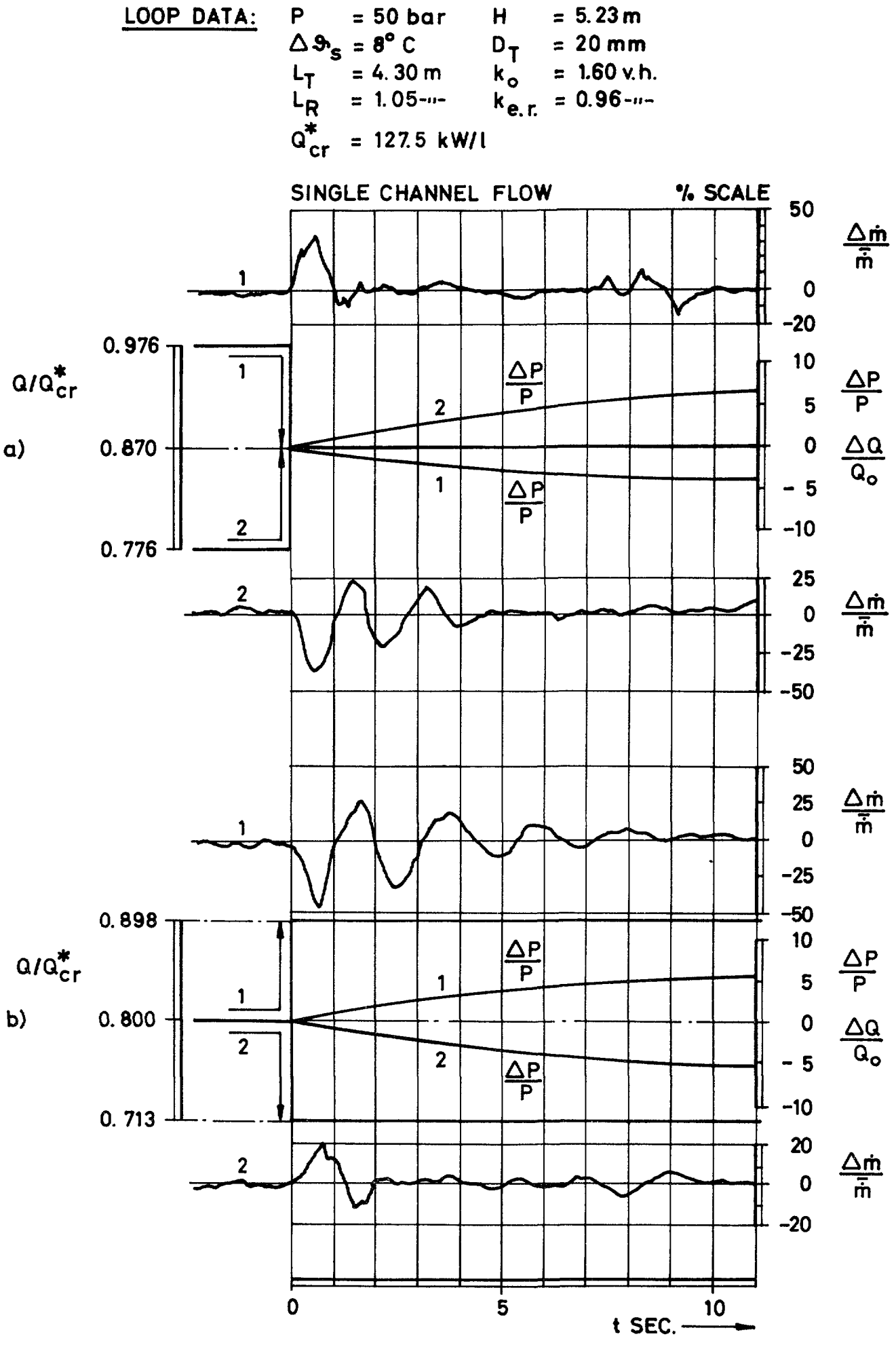

FIG.3 MASS FLOW RESPONSE TO POWER STEP CHANGE.

LOOP DATA: $P = 50$ bar, $H = 5.23$ m, $\Delta\vartheta_s = 8°$ C, $d_T = 20$ mm, $L_T = 4.30$ m, $k_o = 1.60$ v.h., $L_R = 1.05$ -"-, $k_{e.r.} = 0.96$ -"-, $Q^*_{cr} = 127.5$ kW/l

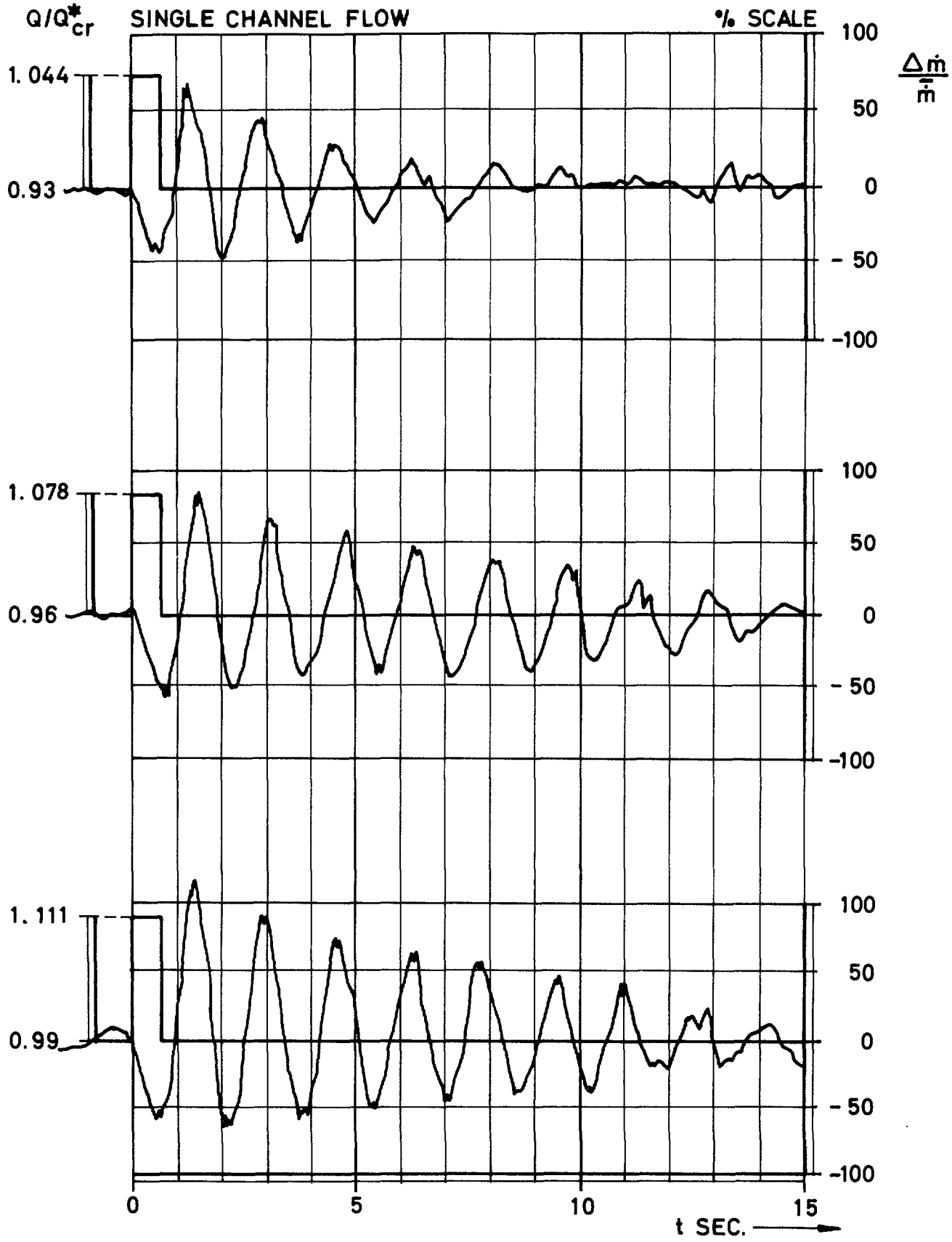

FIG.4 MASS FLOW RESPONSE TO POWER PULSE

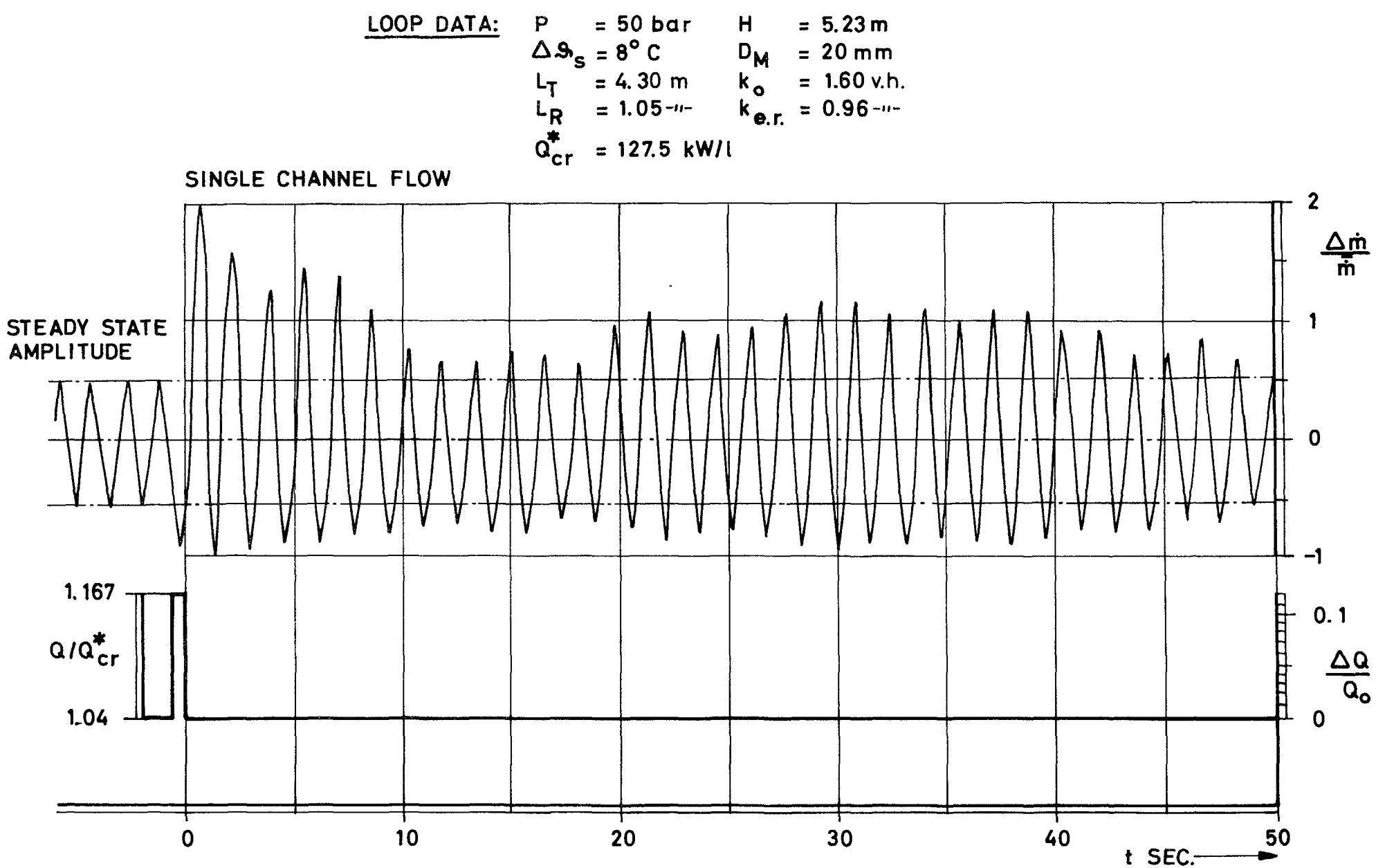

FIG. 5 MASS FLOW RESPONSE TO POWER PULSE WITH INITIALLY UNSTEADY FLOW CONDITIONS

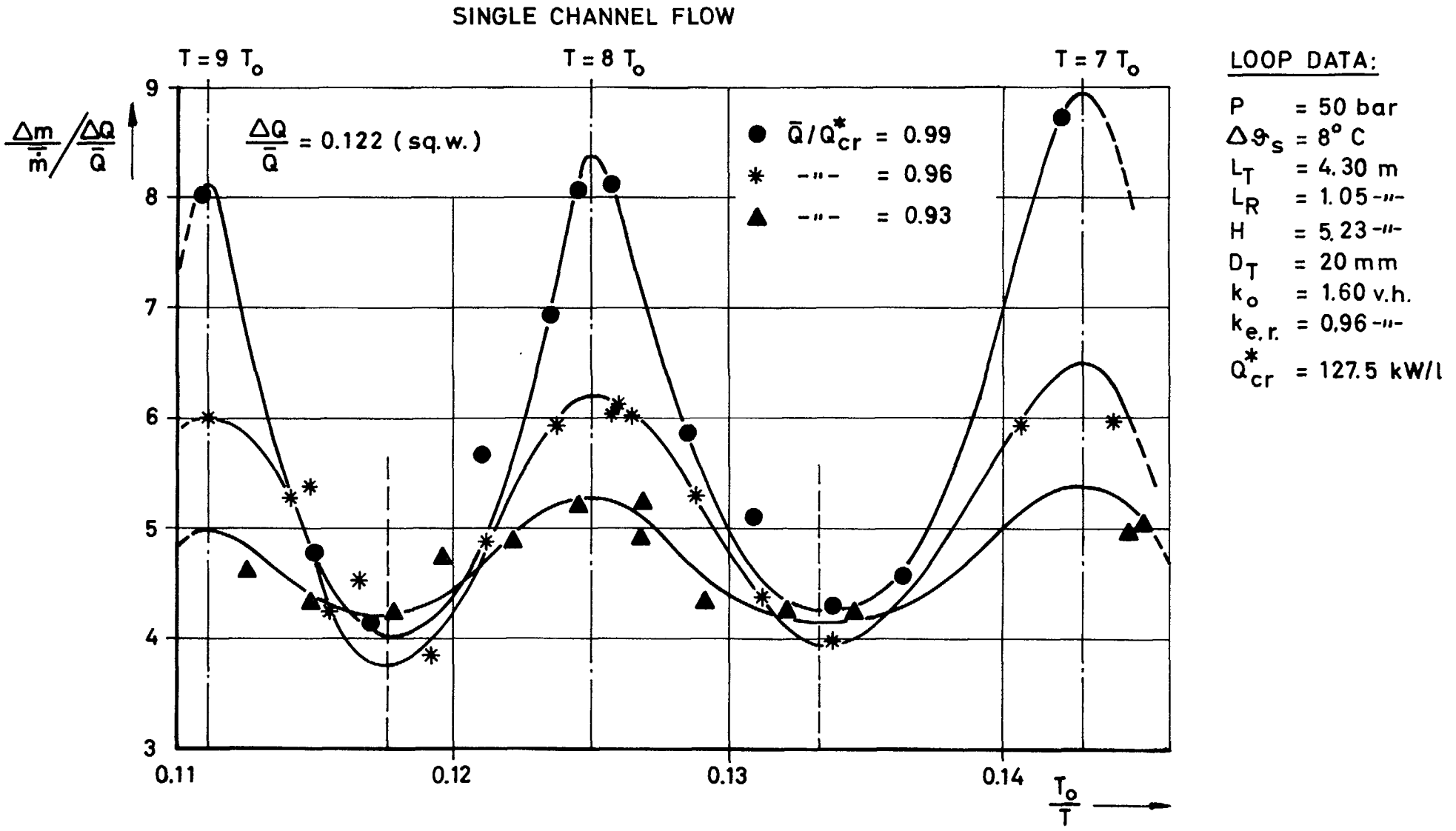

FIG.6 MAXIMUM FLOW RESPONSE AMPLITUDES AT VARYING POWER PULSE INTERVALS

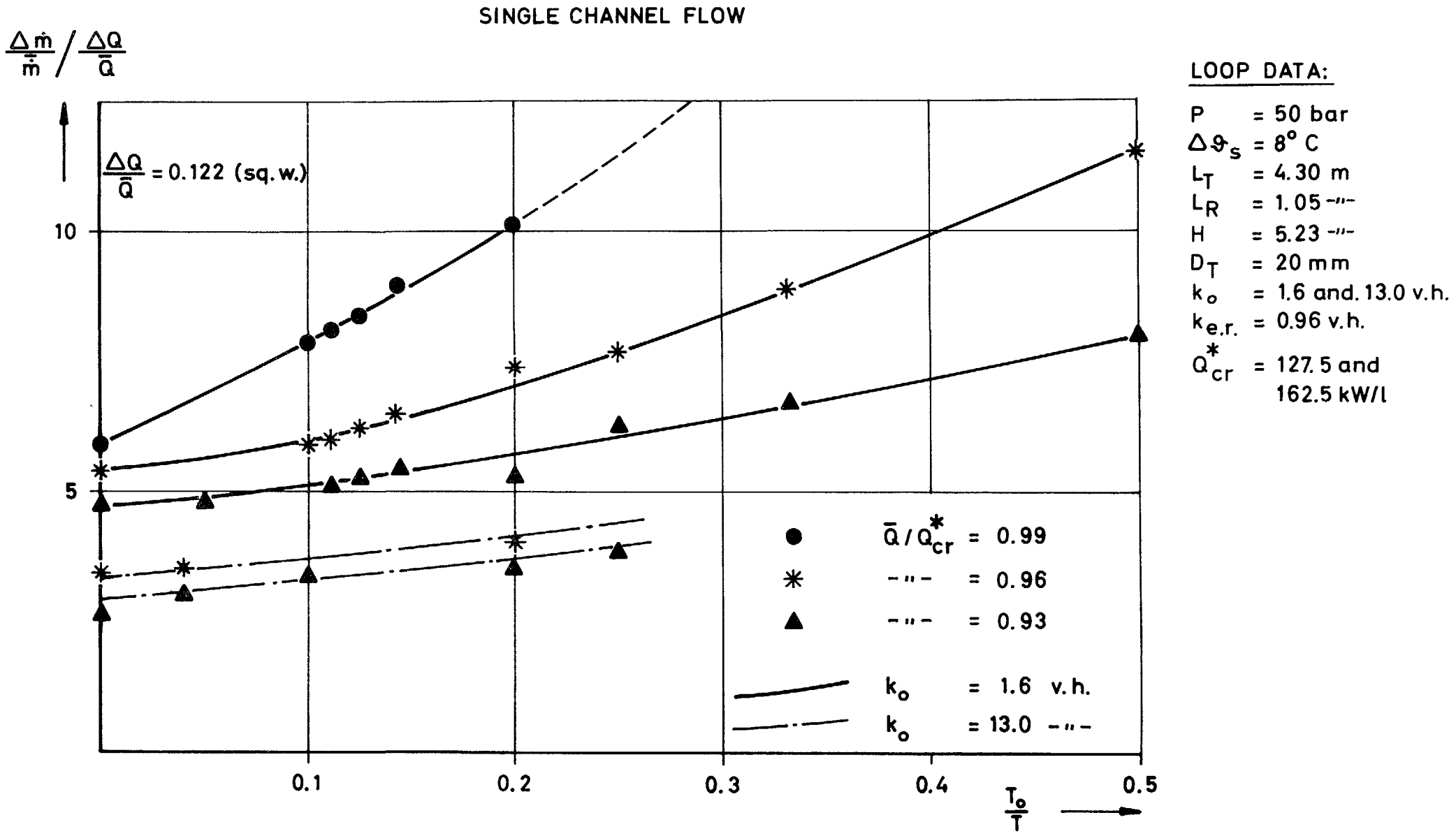

FIG.7 MAXIMUM IMMEDIATE FLOW RESPONSE AMPLITUDES.

LOOP DATA:

P	= 50 bar	H	= 5.23 m
$\Delta\vartheta_s$	= 8° C	D_T	= 20 mm
L_T	= 4.30 m	k_o	= 1.6 and 13.0 v.h.
L_R	= 1.05 -"-	$k_{e.r.}$	= 0.96 v.h.
Q^*_{cr}	= 127.5 and 162.5 kW/l		

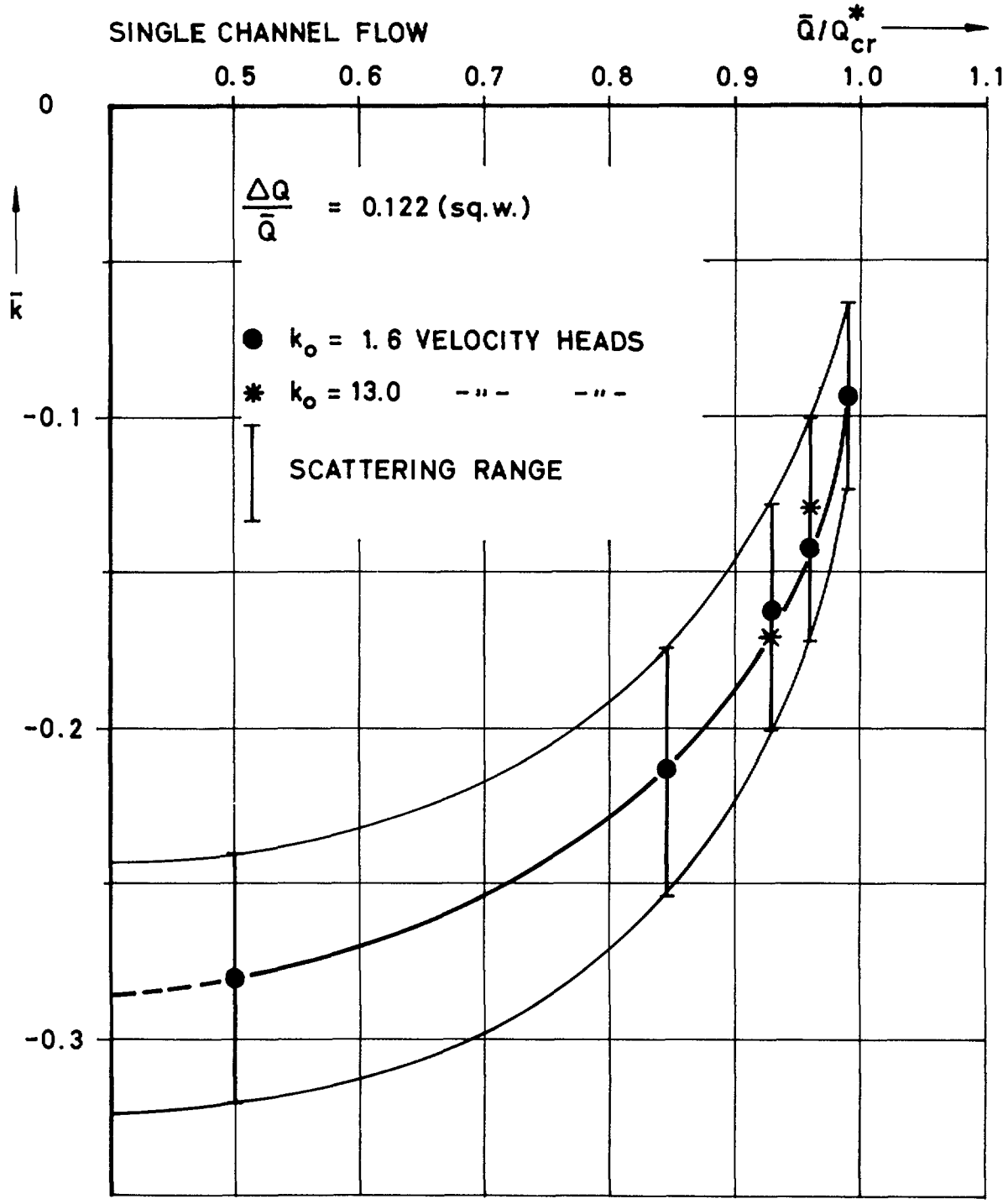

FIG. 8 MEAN DAMPING COEFFICIENT $\bar{k}$ VERSUS $\bar{Q}/Q^*_{cr}$

$$\left[\frac{\Delta\dot{m}}{\dot{\bar{m}}} = \left(\frac{\Delta\dot{m}}{\dot{\bar{m}}}\right)_o \cdot e^{\bar{k}t} \cdot \sin(\omega_o t)\right]$$

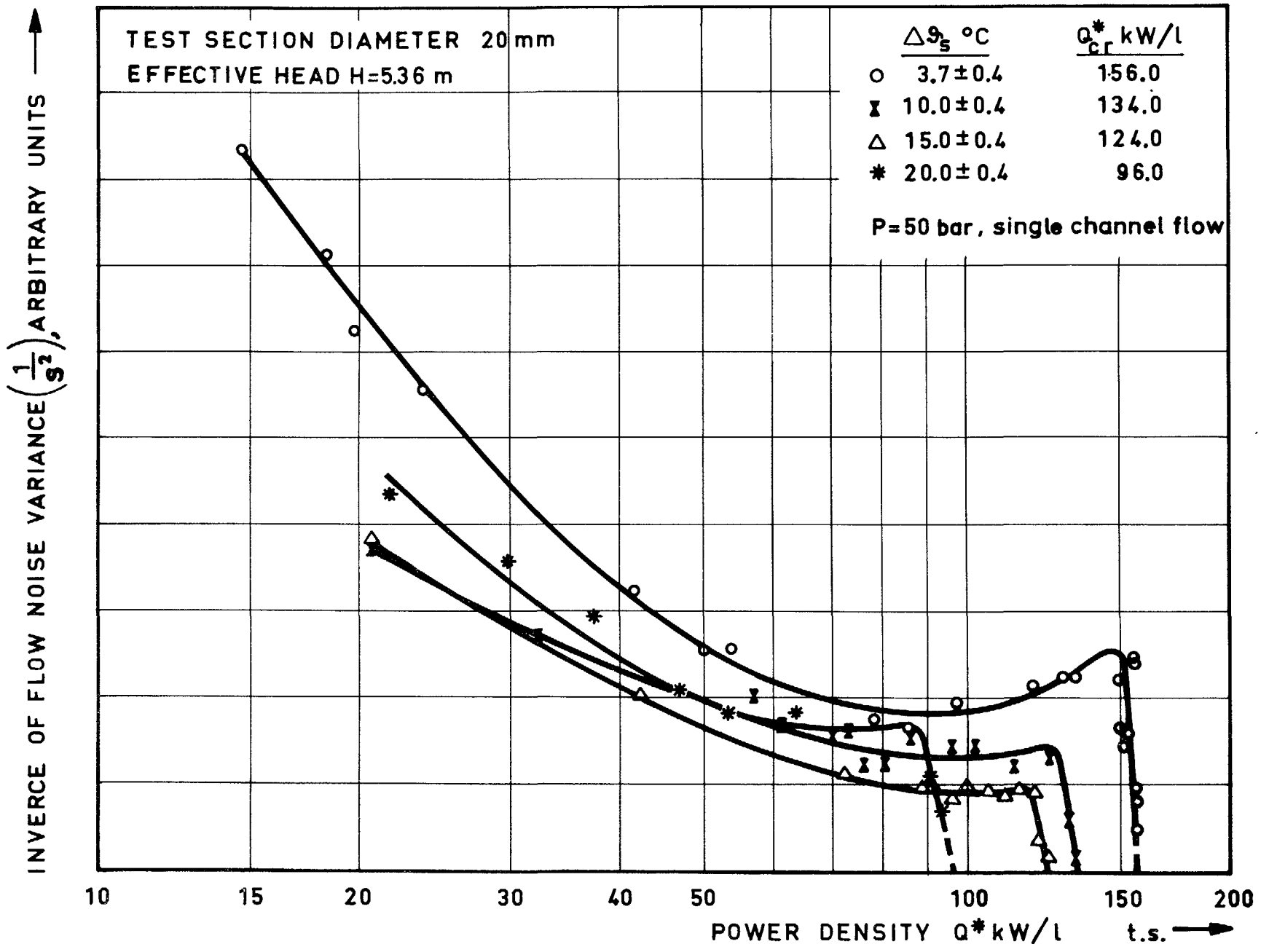

FIG.A1 TYPICAL FLOW NOISE CHARACTERISTICS.

LOOP DATA:

P	= 50 bar	H	= 5.23 m
$\Delta\vartheta_s$	= 6° C	D_T	= 20 mm
L_T	= 4.30m	k_T	= 4.30 v.h.
L_R	= 1.05-"-	$k_{e.r.}$	= 0.96 -"-

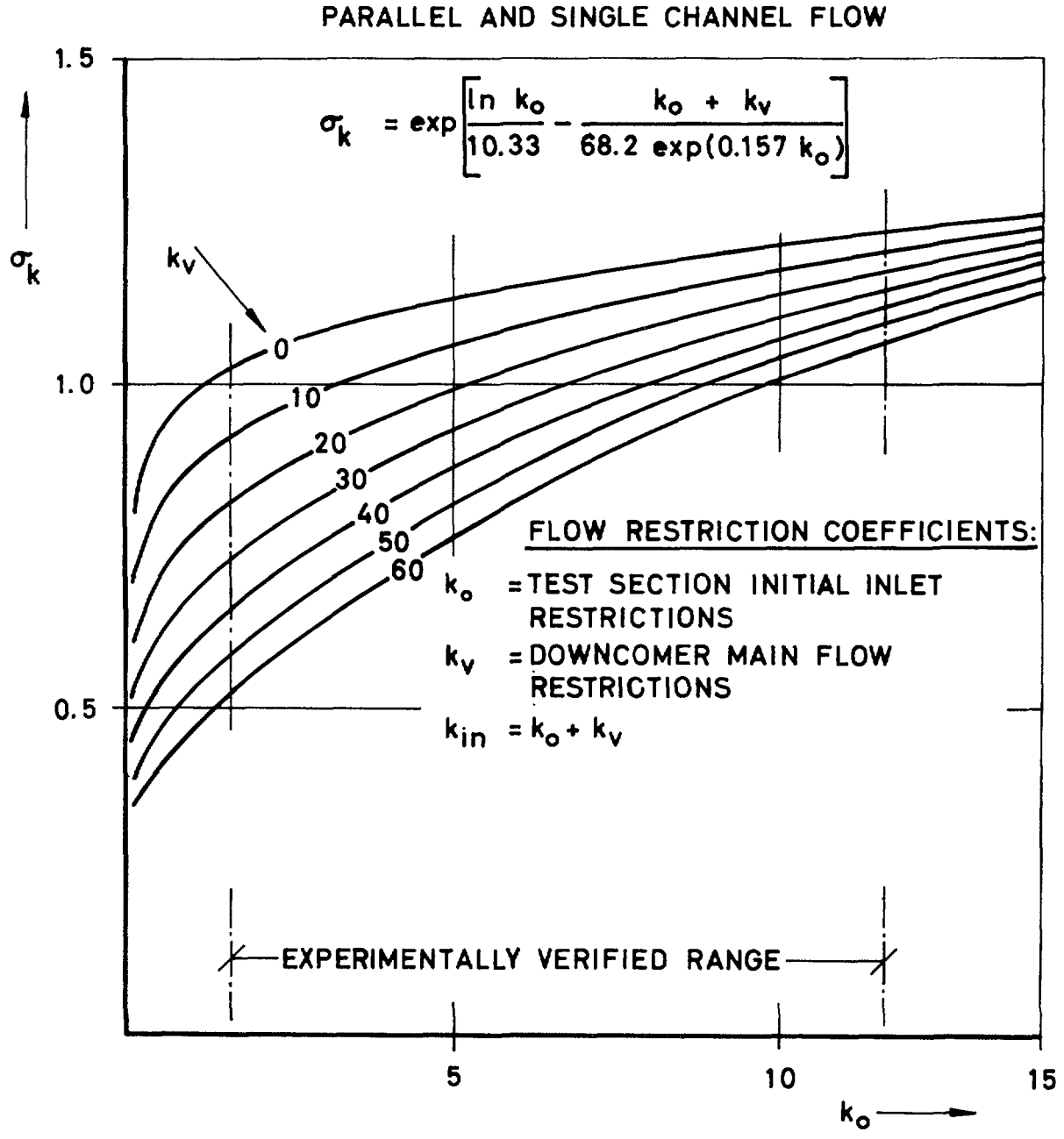

FIG. A2 THE INFLUENCE OF k_o AND k_v ON THE POWER LEVEL AT HYDRODYNAMIC INSTABILITY

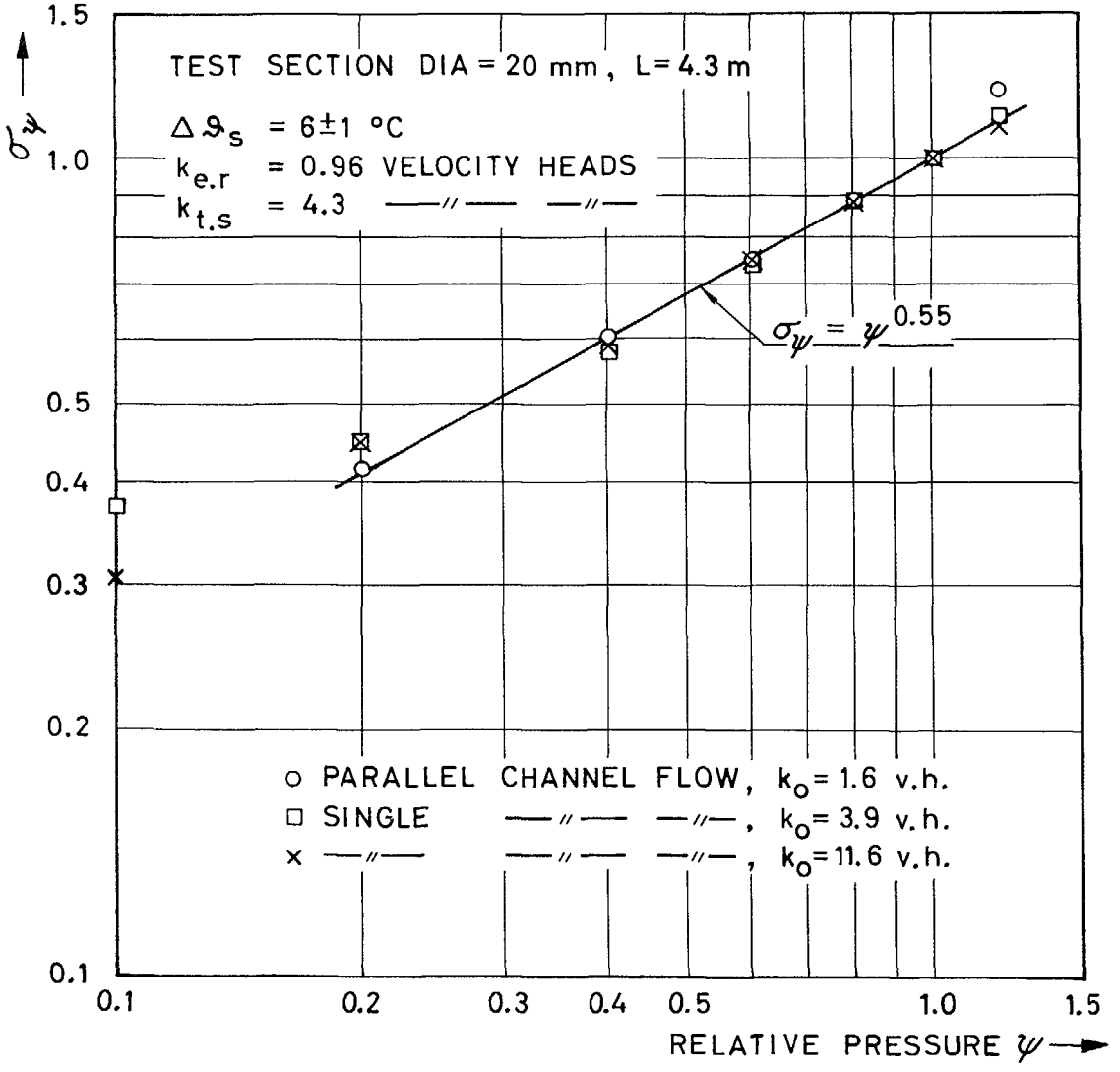

FIG. A3 PRESSURE DEPENDENT POWER FACTOR σ_ψ NORMALIZED TO 50 BAR

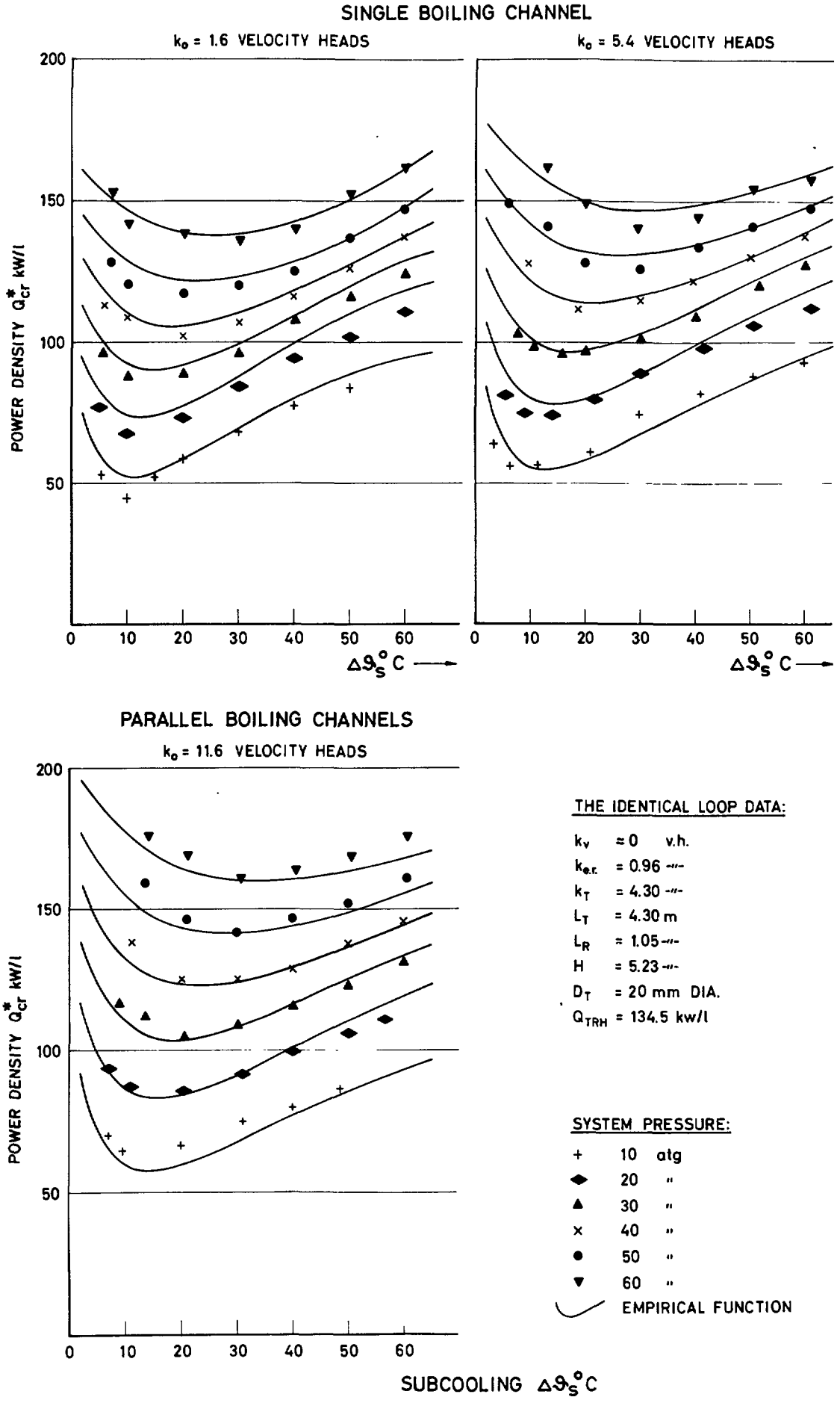

FIG.A4 POWER LEVEL AT HYDRODYNAMIC INSTABILITY IN THE NATURAL CIRCULATION LOOP "SKÄLVAN."

PARALLEL COUPLED ELECTRICAL RESISTANCE RATIO:

$\frac{R'_2}{R'_1} = \frac{(1 + R'_1)a - 1}{(1 + R'_1)(1-a)}$, WHERE $a = \sqrt{\frac{1-p}{1+p}}$ IS THE POWER AMPLITUDE COEFFICIENT.

IN THIS CASE $p = 0.1$

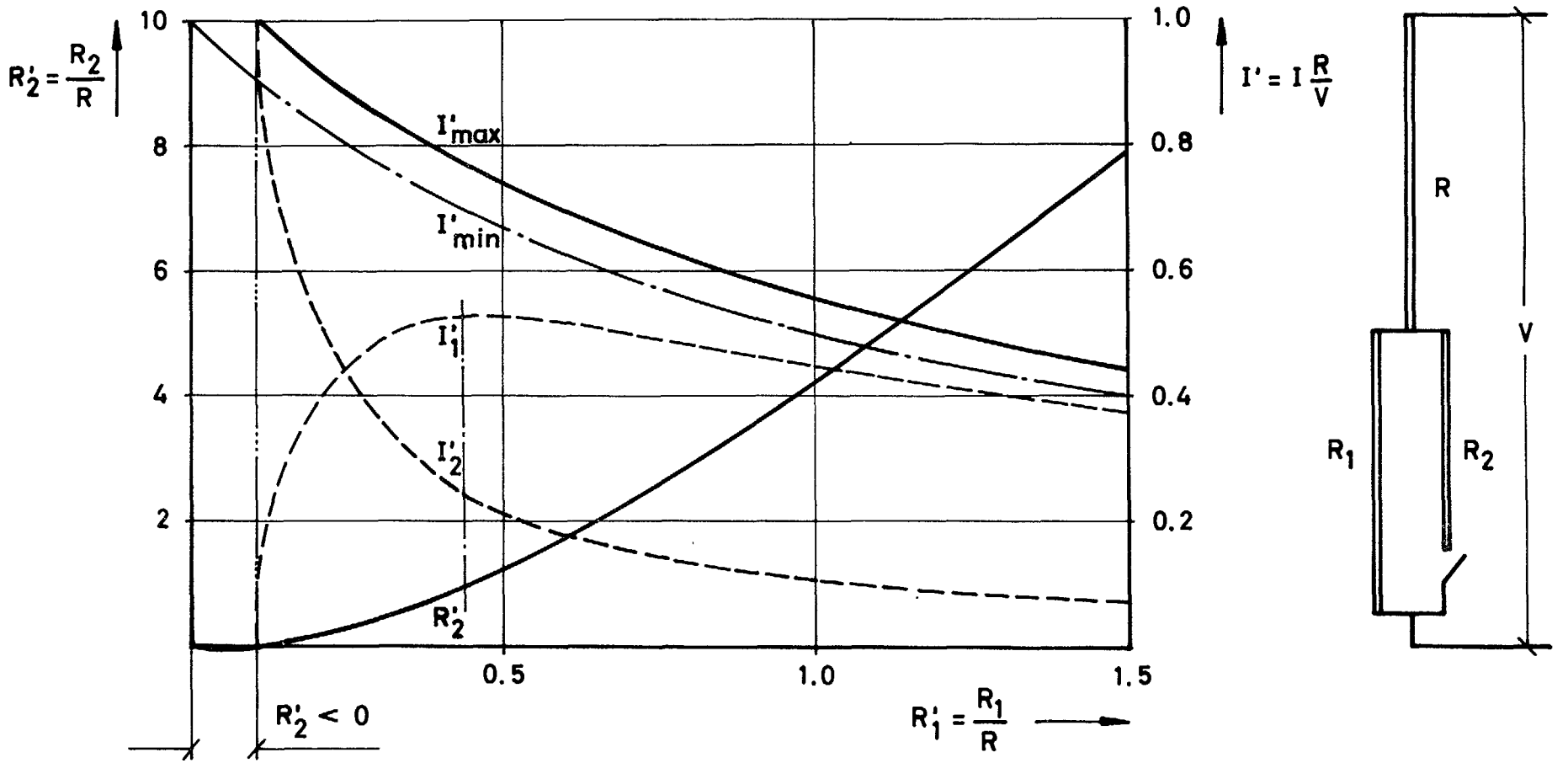

FIG.B1 POWER OSCILLATION SYSTEM. ELECTRICAL CHARACTERISTICS..

LIST OF PUBLISHED AE-REPORTS

1–200. (See the back cover earlier reports.)

201. Heat transfer analogies. By A. Bhattacharyya. 1965. 55 p. Sw. cr. 8:–.

202. A study of the "384" KeV complex gamma emission from plutonium-239. By R. S. Forsyth and N. Ronqvist. 1965. 14 p. Sw. cr. 8:–.

203. A scintillometer assembly for geological survey. By E. Dissing and O. Landström. 1965. 16 p. Sw. cr. 8:–.

204. Neutron-activation analysis of natural water applied to hydrogeology. By O. Landström and C. G. Wenner. 1965. 28 p. Sw. cr. 8:–.

205. Systematics of absolute gamma ray transition probabilities in deformed odd-A nuclei. By S. G. Malmskog. 1965. 60 p. Sw. cr. 8:–.

206. Radiation induced removal of stacking faults in quenched aluminium. By U. Bergenlid. 1965. 11 p. Sw. cr. 8:–.

207. Experimental studies on assemblies 1 and 2 of the fast reactor FR0. Part 2. By E. Hellstrand, T. Andersson, B. Brunfelter, J. Kockum, S-O. Londen and L. I. Tirén. 1965. 50 p. Sw. cr. 8:–.

208. Measurement of the neutron slowing-down time distribution at 1.46 eV and its space dependence in water. By E. Möller. 1965. 29 p. Sw. cr. 8:–.

209. Incompressible steady flow with tensor conductivity leaving a transverse magnetic field. By E. A. Witalis. 1965. 17 p. Sw. cr. 8:–.

210. Methods for the determination of currents and fields in steady two-dimensional MHD flow with tensor conductivity. By E. A. Witalis. 1965. 13 p. Sw. cr. 8:–.

211. Report on the personnel dosimetry at AB Atomenergi during 1964. By K. A. Edvardsson. 1966. 15 p. Sw. cr. 8:–.

212. Central reactivity measurements on assemblies 1 and 3 of the fast reactor FR0. By S-O. Londen. 1966. 58 p. Sw. cr. 8:–.

213. Low temperature irradiation applied to neutron activation analysis of mercury in human whole blood. By D. Brune. 1966. 7 p. Sw. cr. 8:–.

214. Characteristics of linear MHD generators with one or a few loads. By E. A. Witalis. 1966. 16 p. Sw. cr. 8:–.

215. An automated anion-exchange method for the selective sorption of five groups of trace elements in neutron-irradiated biological material. By K. Samsahl. 1966. 14 p. Sw. cr. 8:–.

216. Measurement of the time dependence of neutron slowing-down and thermalization in heavy water. By E. Möller. 1966. 34 p. Sw. cr. 8:–.

217. Electrodeposition of actinide and lanthanide elements. By N-E. Bärring. 1966. 21 p. Sw. cr. 8:–.

218. Measurement of the electrical conductivity of He^3 plasma induced by neutron irradiation. By J. Braun and K. Nygaard. 1966. 37 p. Sw. cr. 8:–.

219. Phytoplankton from Lake Magelungen, Central Sweden 1960–1963. By T. Willén. 1966. 44 p. Sw. cr. 8:–.

220. Measured and predicted neutron flux distributions in a material surrounding av cylindrical duct. By J. Nilsson and R. Sandlin. 1966. 37 p. Sw. cr. 8:–.

221. Swedish work on brittle-fracture problems in nuclear reactor pressure vessels. By M. Grounes. 1966 34 p. Sw. cr. 8:–.

222. Total cross-sections of U, UO_2 and ThO_2 for thermal and subthermal neutrons. By S. F. Beshai. 1966. 14 p. Sw. cr. 8:–.

223. Neutron scattering in hydrogenous moderators, studied by the time dependent reaction rate method. By L. G. Larsson, E, Möller and S. N. Purohit. 1966. 26 p. Sw. cr. 8:–.

224. Calcium and strontium in Swedish waters and fish, and accumulation of strontium-90. By P-O. Agnedal. 1966. 34 p. Sw. cr. 8:–.

225. The radioactive waste management at Studsvik. By R. Hedlund and A. Lindskog. 1966. 14 p. Sw cr. 8:–.

226. Theoretical time dependent thermal neutron spectra and reaction rates in H_2O and D_2O. S. N. Purohit. 1966. 62 p. Sw. cr. 8:–.

227. Integral transport theory in one-dimensional geometries. By I. Carlvik. 1966. 65 p. Sw. cr. 8:–.

228. Integral parameters of the generalized frequency spectra of moderators. By S. N. Purohit. 1966. 27 p. Sw. cr. 8:–.

229. Reaction rate distributions and ratios in FR0 assemblies 1, 2 and 3. By T. L. Andersson. 1966. 50 p. Sw. cr. 8:–.

230. Different activation techniques for the study of epithermal spectra, applied to heavy water lattices of varying fuel-to-moderator ratio. By E. K Sokolowski. 1966. 34 p. Sw. cr. 8:–.

231. Calibration of the failed-fuel-element detection systems in the Ågesta reactor. By O. Strindehag. 1966. 52 p. Sw. cr. 8:–.

232. Progress report 1965. Nuclear chemistry. Ed. by G. Carleson. 1966. 26 p. Sw. cr. 8:–.

233. A summary report on assembly 3 of FR0. By T. L. Andersson, B. Brunfelter, P. F. Cecchi, E. Hellstrand, J. Kockum, S-O. Londen and L. I Tirén. 1966. 34 p. Sw. cr. 8:–

234. Recipient capacity of Tvären, a Baltic Bay. By P.-O. Agnedal and S. O. W. Bergström. 1966. 21 p. Sw. cr. 8:–.

235. Optimal linear filters for pulse height measurements in the presence of noise. By K. Nygaard. 1966. 16 p. Sw. cr. 8:–.

236. DETEC, a subprogram for simulation of the fast-neutron detection process in a hydro-carbonous plastic scintillator. By B. Gustafsson and O. Aspelund. 1966. 26 p. Sw. cr. 8:–.

237. Microanalys of fluorine contamination and its depth distribution in zircaloy by the use of a charged particle nuclear reaction. By E. Möller and N. Starfelt. 1966. 15 p. Sw. cr. 8:–.

238. Void measurements in the regions of sub-cooled and low-quality boiling. P. 1. By S. Z. Rouhani. 1966. 47 p. Sw. cr. 8:–.

239. Void measurements in the regions of sub-cooled and low-quality boiling. P. 2. By S. Z. Rouhani. 1966. 60 p. Sw. cr. 8:–.

240. Possible odd parity in ^{128}Xe. By L. Broman and S. G. Malmskog. 1966. 10 p. Sw. cr. 8:–.

241. Burn-up determination by high resolution gamma spectrometry: spectra from slightly-irradiated uranium and plutonium between 400–830 keV. By R. S. Forsyth and N. Ronqvist. 1966. 22 p. Sw. cr. 8:–.

242. Half life measurements in ^{155}Gd. By S. G. Malmskog. 1966. 10 p. Sw. cr. 8:–.

243. On shear stress distributions for flow in smooth or partially rough annuli. By B. Kjellström and S. Hedberg. 1966. 66 p. Sw. cr. 8:–.

244. Physics experiments at the Ågesta power station. By G. Apelqvist, P.-Å. Bliselius, P. E. Blomberg, E. Jonsson and F. Åkerhielm. 1966. 30 p. Sw. cr. 8:–.

245. Intercrystalline stress corrosion cracking of inconel 600 inspection tubes in the Ågesta reactor. By B. Grönwall, L. Ljungberg, W. Hübner and W. Stuart. 1966. 26 p. Sw. cr. 8:–.

246. Operating experience at the Ågesta nuclear power station. By S. Sandström. 1966. 113 p. Sw. cr. 8:–.

247. Neutron-activation analysis of biological material with high radiation levels By K. Samsahl. 1966. 15 p. Sw. cr. 8:–.

248. One-group perturbation theory applied to measurements with void. By R Persson. 1966. 19 p. Sw. cr. 8:–.

249. Optimal linear filters. 2. Pulse time measurements in the presence of noise. By K. Nygaard. 1966 9 p. Sw. cr. 8:–.

250. The interaction between control rods as estimated by second-order one-group perturbation theory. By R. Persson. 1966. 42 p. Sw. cr. 8:–.

251. Absolute transition probabilities from the 453.1 keV level in 183W. By S. G Malmskog. 1966. 12 p. Sw. cr. 8:–.

252. Nomogram for determining shield thickness for point and line sources of gamma rays. By C. Jönemalm and K. Malén. 1966. 33 p. Sw. cr. 8:–

253. Report on the personnel dosimetry at AB Atomenergi during 1965. By K. A Edwardsson. 1966. 13 p. Sw. cr. 8:–.

254 Buckling measurements up to 250°C on lattices of Ågesta clusters and on D_2O alone in the pressurized exponential assembly TZ. By R. Persson, A. J. W. Andersson and C.-E. Wikdahl. 1966. 56 p. Sw. cr. 8:–.

255 Decontamination experiments on intact pig skin contaminated with beta-gamma-emitting nuclides. By K. A. Edwardsson, S. Hagsgård and Å. Swensson. 1966. 35 p. Sw. cr. 8:–.

256. Perturbation method of analysis applied to substitution measurements of buckling. By R. Persson. 1966. 57 p. Sw. cr. 8:–.

257. The Dancoff correction in square and hexagonal lattices. By I. Carlvik. 1966 35 p. Sw. cr. 8:–.

258. Hall effect influence on a highly conducting fluid. By E. A. Witalis. 1966 13 p. Sw. cr. 8:–.

259. Analysis of the quasi-elastic scattering of neutrons in hydrogenous liquids By S. N. Purohit. 1966. 26 p. Sw. cr. 8:–.

260 High temperature tensile properties of unirradiated and neutron irradiated 20Cr–35Ni austenitic steel By R B Roy and B Solly. 1966. 25 p. Sw cr. 8:–.

261. On the attenuation of neutrons and photons in a duct filled with a helical plug. By E. Aalto and Å. Krell. 1966. 24 p. Sw. cr. 8:–.

262. Design and analysis of the power control system of the fast zero energy reactor FR-0. By N. J. H. Schuch. 1966. 70 p. Sw. cr. 8:–.

263. Possible deformed states in ^{115}In and ^{117}In. By A. Bäcklin, B. Fogelberg and S. G. Malmskog. 1967. 39 p. Sw. cr. 10:–.

264. Decay of the 16.3 min. ^{182}Ta isomer. By M. Höjeberg and S. G. Malmskog. 1967. 13 p. Sw. cr. 10:–.

265. Decay properties of ^{147}Nd. By A. Bäcklin and S. G. Malmskog. 1967. 15 p. Sw. cr. 10: –.

266. The half life of the 53 keV level in ^{197}Pt. By S. G. Malmskog. 1967. 10 p. Sw. cr. 10:–.

267. Burn-up determination by hight resolution gamma spectrometry: Axial and diametral scanning experiments. By R. S. Forsyth, W. H. Blackadder and N. Ronqvist. 1967. 18 p. Sw. cr. 10:–.

268. On the properties of the $s_{1/2} \longrightarrow d_{3/2}$ transition in ^{199}Au. By A. Bäcklin and S. G. Malmskog. 1967. 23 p. Sw. cr. 10:–.

269. Experimental equipment for physics studies in the Ågesta reactor. By G. Bernander, P. E. Blomberg and P.-O. Dubois. 1967. 35 p. Sw. cr. 10:–.

270. An optical model study of neutrons elastically scattered by iron, nickel, cobalt, copper, and indium in the energy region 1.5 to 7.0 MeV. By B. Holmqvist and T. Wiedling. 1967. 20 p. Sw. cr. 10:–.

271. Improvement of reactor fuel element heat transfer by surface roughness. By B. Kjellström and A. E. Larsson. 1967. 94 p. Sw. cr. 10:–.

272. Burn-up determination by high resolution gamma spectormetry Fission product migration studies. By R. S. Forsyth, W. H. Blackadder and N. Ronqvist. 1967. 19 p. Sw. cr. 10:–.

273. Monoenergetic critical parameters and decay constants for small spheres and thin slabs. By I. Carlvik. 24 p. Sw. cr. 10:–.

274. Scattering of neutrons by an anharmonic crystal. By T. Högberg, L. Bohlin and I. Ebbsjö. 1967. 38 p. Sw. cr. 10:–.

275. The $|\Delta K|=1$, E1 transitions in odd-A isotopes of Tb and Eu. By S. G. Malmskog, A. Marelius and S. Wahlborn. 1967. 24 p. Sw. cr. 10:–.

276. A burnout correlation for flow of boiling water in vertical rod bundles. By Kurt M. Becker. 1967. 102 p. Sw. cr. 10:–.

277. Epithermal and thermal spectrum indices in heavy water lattices. By E. K. Sokolowski and A. Jonsson. 1967. 44 p. Sw. cr. 10:–.

278. On the $d_{5/2} \leftrightarrow g_{7/2}$ transitions in odd mass Pm nuclei. By A. Bäcklin and S. G. Malmskog. 1967. 14 p. Sw. cr. 10:–.

279. Calculations of neutron flux distributions by means of integral transport methods. By I. Carlvik. 1967. 94 p. Sw. cr. 10:–.

280. On the magnetic properties of the K=1 rotational band in ^{185}Re. By S. G. Malmskog and M. Höjeberg. 1967. 18 p. Sw. cr. 10:–.

281. Collision probabilities for finite cylinders and cuboids. By I. Carlvik. 1967. 28 p. Sw. cr. 10:–.

282. Polarized elastic fast-neutron scattering off ^{12}C in the lower MeV-range. I. Experimental part. By O. Aspelund. 1967. 50 p. Sw. cr. 10:–.

283. Progress report 1966 nuclear chemistry. 1967. 26 p. Sw. cr. 10:–.

284. Finite-geometry and polarized multiple-scattering corrections of experimental fast-neutron polarization data by means of Monte Carlo methods. By O. Aspelund and B. Gustafsson. 1967. 60 p. Sw. cr. 10:–.

285. Power disturbances close to hydrodynamic instability in natural circulation two-phase flow. By R. P. Mathisen and O. Eklind. 1967. 34 p. Sw. cr. 10:–.

Förteckning över publicerade AES-rapporter

1. Analys medelst gamma-spektrometri. Av D. Brune. 1961. 10 s. Kr 6:–.
2. Bestrålningsförändringar och neutronatmosfär i reaktortrycktankar – några synpunkter. Av M. Grounes. 1962. 33 s. Kr 6:–.
3. Studium av sträckgränsen i mjukt stål. Av G. Östberg och R. Attermo 1963. 17 s. Kr 6:–.
4. Teknisk upphandling inom reaktorområdet. Av Erik Jonson. 1963. 64 s. Kr 8:–.
5. Ågesta Kraftvärmeverk. Sammanställning av tekniska data, beskrivningar m. m. för reaktordelen. Av B. Lilliehöök. 1964. 336 s. Kr 15:–.
6. Atomdagen 1965. Sammanställning av föredrag och diskussioner. Av S. Sandström. 1966. 321 s. Kr 15:–.

Additional copies available at the library of AB Atomenergi, Studsvik, Nyköping, Sweden. Micronegatives of the reports are obtainable through Filmprodukter, Gamla landsvägen 4, Ektorp, Sweden.

EOS-tryckerierna, Stockholm 1967